

IPNO DRE 94-06 /

PROJECTILE FISSION OF ^{238}U RELATIVISTIC IONS IN A Pb TARGET AND DISCOVERY OF NEW FISSION FRAGMENTS.

M. Bernas, C. Donzaud, C. Stéphan, L. Tassan-Got,
IPN, Orsay, France

S. Czajkowski, P. Armbruster, H. Geissel, C. Korzuharov,
G. Münzenberg, K.H. Schmidt, W. Schwab, K. Summerer,
M. Pfützner, GSI, Darmstadt, Germany

Ph. Dessagne, Ch. Mische, CRN, Strasbourg, France

H.R. Faust, M. Hesse, ILL, Grenoble, France

E. Hanelt, A. Heinz, C. Röhl, B. Voss, TH Darmstadt, Germany

XXXIInd Winter Meeting, Bormio (1994)

IPNO DRE 94-06 /

**PROJECTILE FISSION OF ^{238}U RELATIVISTIC IONS IN A Pb
TARGET AND DISCOVERY OF NEW FISSION FRAGMENTS.**

M. Bernas, C. Donzaud, C. Stéphan, L. Tassan-Got,
IPN, Orsay, France

S. Czajkowski, P. Armbruster, H. Geissel, C. Korzhuharov,
G. Münzenberg, K.H. Schmidt, W. Schwab, K. Summerer,
M. Pfützner, GSI, Darmstadt, Germany

Ph. Dessagne, Ch. Mische, CRN, Strasbourg, France

H.R. Faust, M. Hesse, ILL, Grenoble, France

E. Hanelt, A. Heinz, C. Röhl, B. Voss, TH Darmstadt, Germany

XXXII^d Winter Meeting, Bormio (1994)

Projectile fission of ^{238}U relativistic ions in a Pb target and discovery of new fission fragments.

M. Bernas¹, S. Czajkowski², P. Armbruster², H. Geissel², Ph. Dessagne³, C. Donzaud¹, H-R. Faust⁴, E. Hanelt⁵, A. Heinz⁵, M. Hesse⁴, C. Kozhuharov², Ch. Miehe³, G. Münzenberg², M. Pfützner², C. Röhl⁵, K.-H. Schmidt², W. Schwab², C. Stéphan¹, K. Sümmerner², L. Tassan-Got¹, B. Voss⁵.

¹IPN Orsay, ²GSI Darmstadt, ³CRN Strasbourg, ⁴ILL Grenoble,

⁵TH Darmstadt

Neutron-rich nuclei have to be investigated in order to extend the field of spectroscopy and to improve the nuclear models. Their properties as binding energy, half-life, β -decay scheme and probability of neutron emission are required to calculate the r-process and to reproduce the mass distribution observed in the solar system. Fission has been for the previous 20 years the most efficient source of neutron-rich isotopes [1].

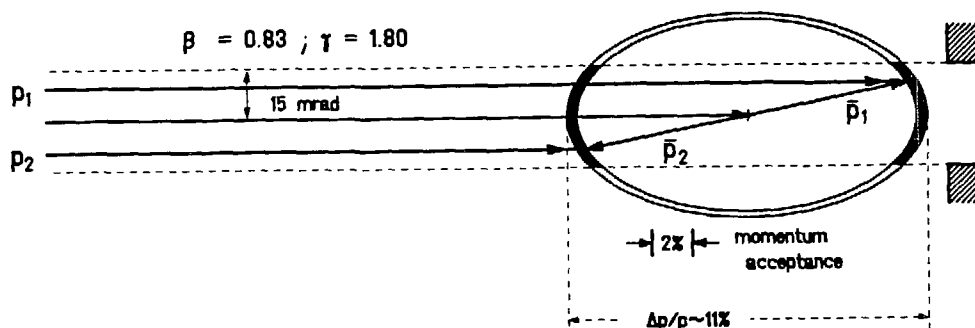
With the ^{238}U beam recently accelerated at relativistic energies by the heavy ion synchrotron (SIS) at GSI, fission was investigated using inverse kinematics. This geometry is well suited for analyzing fragments with the fragment separator FrS. The fragments resulting from peripheral collisions are forward emitted, with similar velocities hence they are efficiently transmitted in the FrS. The transmission is multiplied by more than 5 orders of magnitude as compared with values obtained with fission products recoil separators [2]. An other major advantage offered by the high velocity of the fragments is their complete ionization. For neutron-rich studies this point is crucial since magnet deflection of charge states of abundant isotopes would be the same as for the fully stripped rare fragments of interest. At last, high velocity fission fragments selected with the FrS can be identified with energy loss and time of flight measurements.

A 750 A.MeV U beam of 10^6 nuclei/spill was impinging on a 1.25 gr/cm² Pb target. Fragments were separated and analyzed with the FrS [3]. This last generation separator, designed after the Bevalac separator at LBL [4] and the LISE spectrometer in Ganil [5], consists of 2 sets of 2 dipoles, symmetric versus an intermediate dispersive focal plane. It provides optimum optical qualities and versatility. Its performances are well illustrated in the following.

The fragments are identified by in flight measurements of their energy loss (ΔE) and time of flight (ToF) signals. For a given velocity, a Bp scanning of the fragments gives a survey of production cross-sections in terms of A/Z.

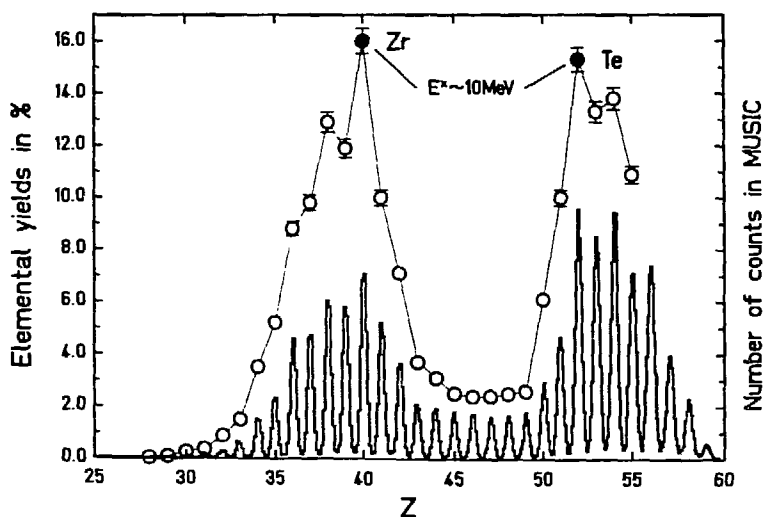
Projectile fission and projectile fragmentation shows different kinematics. The velocity given by the exoenergetic fission process ($\beta_f = 0.05$) must be added relativistically to the projectile velocity ($\beta_p = 0.8$)(see Fig.1). The resulting

Fig 1 Momentum diagram of fission in relativistic inverse kinematics. Forward and backward emitted fragments are indicated in black.



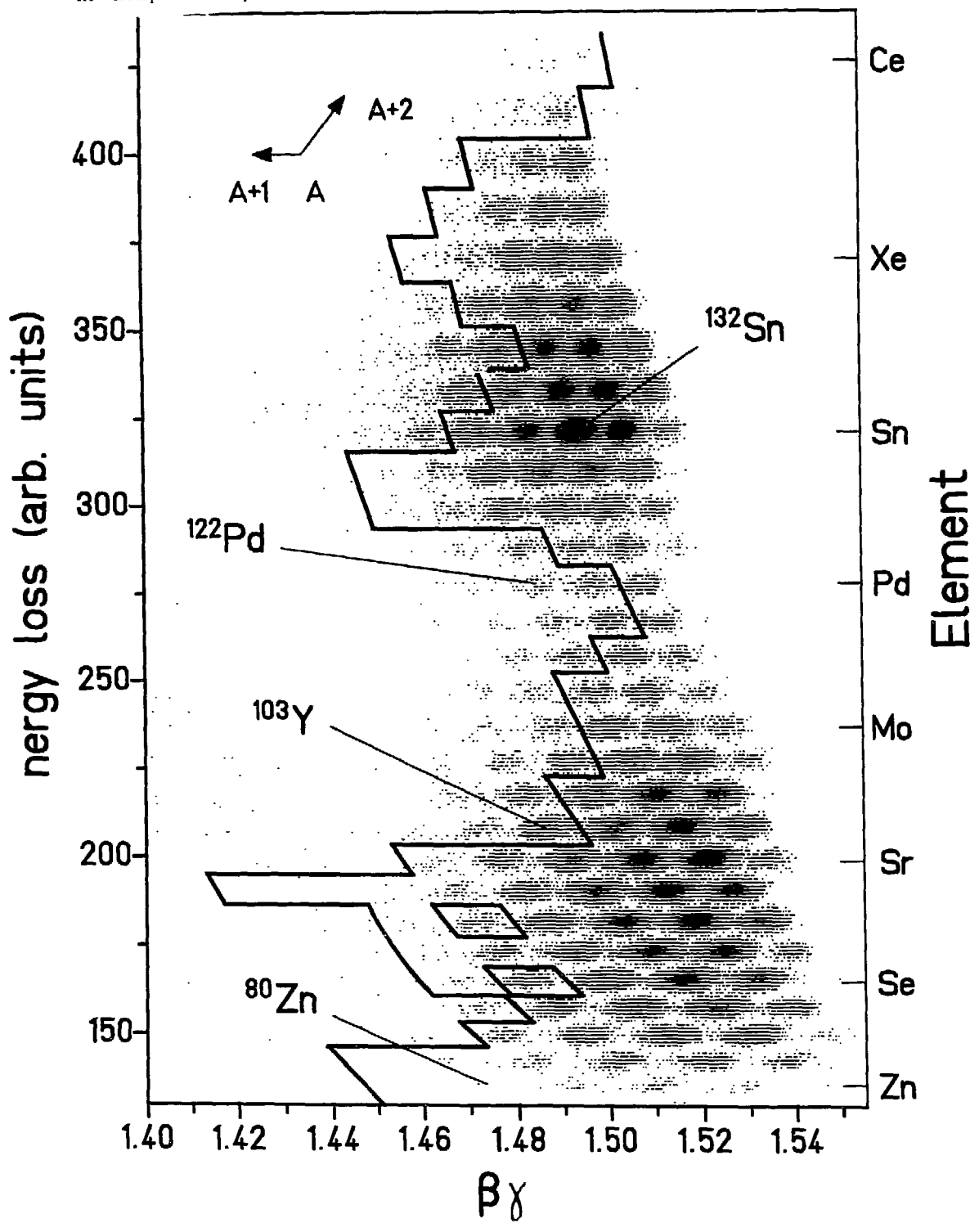
laboratory velocities are distributed in a cone of 60 mr angular aperture. The FrS angular acceptance of 30 mr introduces a cut in the phase space of the fragments, and either forward or backward emitted ions are transmitted in the magnet system. Since the two groups of fragments have momenta 11% apart, they are not simultaneously analyzed by the FrS, the momentum acceptance of which is only 2%. The 1.25 gr cm^2 thick target introduces a "location straggling" effect on the momenta of the fragments of approximately 3%, washing out the energy fluctuations of the fission process and the energy spread due to the opening angle of the FrS (0.7%).

Fig 2 Elemental yields measured in 750 A MeV ^{238}U fission on Pb target for a magnetic rigidity of $1.03 \cdot (B\rho)_0$



The distribution of elements measured at the final image plane of the FrS with the MUSIC ionization chamber [5] is shown on Fig.2. The magnetic rigidity was set to a value 3% larger than $(B\rho)_0$, the projectile magnetic rigidity in the FrS after the target. For

Fig 3 ΔE -Tof scatter-plot of fission fragments observed at $1.08 \times (B\rho)_0$ During the 10 hours irradiation 3.10^5 events were recorded. The full line indicates the present limit of known isotopes. On the left of it, many of the new isotopes are clearly visible. Some isotopes are indicated for orientation

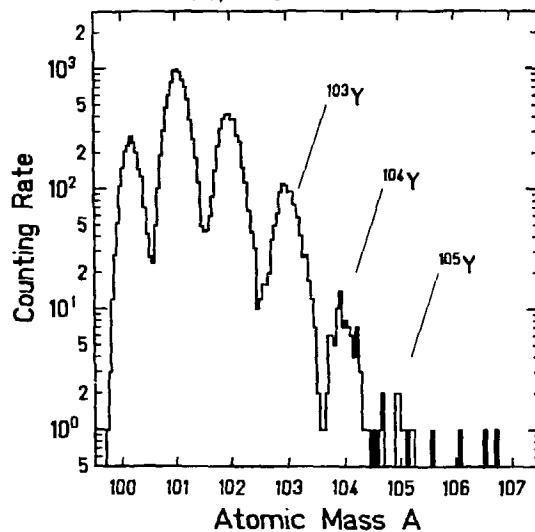


this setting, fission products at maximum yield are transmitted through the magnets. When corrected for the velocity dependence, the measured elemental distribution shows a Z resolution of 1/40 appropriate to isolate each element up to the largest Z . The double humped shape of this distribution, characteristic of low energy fission, is clearly observed. Furthermore an odd-even effect of a few percent is seen in the region of Zr and Te. At small and large Z values, a cut in the FrS transmission is visible. It comes from the 5 mm scintillator located in the intermediate dispersive focal plane (start of the ToF measurement) which introduces an energy loss selection. During this experiment, the FrS was tuned on the light group of fission fragments, $Z=40$. Thus fragments with $Z=30$ and 50 were not well transmitted. The Z calibration was extrapolated from U energy loss measurement and confirmed by the finding of enhanced yields for the Zr-Te pair as known from low energy fission.

From the time of flight of the fragments measured along the second half of the separator, namely 37 m, the velocity was deduced. When the rigidity $B\rho$ and Z are known, the absolute value of the mass A can be calculated. However, a good accuracy is required to achieve a mass resolution better than 1/200 at relativistic energies. The ToF accuracy obtained here was 1/1000, and including detailed information on the trajectories a comparable precision could be achieved on $B\rho$, leading to a mass resolution of 1/250. An illustration of the performances of the FrS equipped with the MUSIC chamber and the ToF scintillators is given on Fig.3. On this scatter-plot the isotopes are clearly separated up to the largest Z (cerium). On Fig.4 the projection of the Y isotopic yields shows the mass resolution. The absolute values of the mass number were obtained by an event-by-event calculation of $A = f(B\rho, \text{ToF})$ for a given Z .

The plot reported on Fig.3 corresponds to a magnetic rigidity $B\rho = 1.08 \cdot (B\rho)_0$ where $(B\rho)_0$ is the value for the U projectile after the target. It is the maximum rigidity for which fission fragments can still be separated at the present beam intensity. Forward emitted fission fragments have almost the same velocities, hence largest A/Z .

Fig. 4 Count rate distribution for Y measured as in Fig. 3. New isotopes are indicated



isotopes are obtained at this setting. Indeed a number of unknown isotopes are observed on this plot. The frontier of reported isotopes [6] is indicated by the solid line and the new species are seen on the left of this line

A list of the new isotopes is given in table 1 together with the number of counts. The related cross-sections have been calculated using transmission of the FrS simulated with a Monte Carlo code MOCADI[7]. In parenthesis are given observed isotopes with low counting rates which should be confirmed by better statistics. They are populated with cross-sections of approximately 1 μb which is the present limit of measured cross sections. The new isotopes are filling the gap of elements not accessible to chemistry or to ISOL ion source techniques. 3 to 4 new isotopes/element are observed in the region of the fission valley; where yields are presently much higher than in low energy fission. The last n-rich isotopes investigated recently in this region were produced by fission induced by 20 MeV protons and separated by using the IGISOL facility [8] Not only a new land of fragments is revealed, but it is the first ΔE -ToF isotopic identification of heavy fission fragments. It provides accurate relative yields free from chemical or radio-chemical bias. One should note also on Fig.3 the enhanced yield for ^{132}Sn which was counted with a rate of one event/s. Secondary beams of fission fragments can be separated as in case of any other projectile fragment [9].

Table 1 List of the new isotopes and of the number of counts observed in a setting of the FrS corresponding to $1.08^*(\text{Bp})_0$. Cross-sections evaluated as described in the text are given. Uncertainties of 30 to 40% include statistical errors and transmission uncertainties

Isotope	Counts	$\sigma(\mu\text{b})$	Isotope	Counts	$\sigma(\mu\text{b})$	Isotope	Counts	$\sigma(\mu\text{b})$	Isotope	Counts	$\sigma(\mu\text{b})$
^{86}Ge	10	7	^{111}Mo	135	66	^{122}Pd	79	25	^{142}Te	5	
^{88}As	51	31	^{112}Mo	29	15	^{123}Pd	12	4	^{143}I	49	15
^{89}As	8	5	$^{(113}\text{Mo)}$	3	2	^{125}Ag	119	37	^{144}I	7	3
^{90}Se	409	240	^{114}Tc	53	24	^{126}Ag	19	6	$^{(147}\text{Xe)}$	4	1
^{98}Kr	155	88	^{115}Tc	18	9	^{135}Sn	193	63	^{151}Ba	13	4
^{103}Y	972	490	^{116}Ru	168	63	^{136}Sn	34	12	^{151}La	106	>52
^{104}Y	94	48	^{117}Ru	30	11	$^{(137}\text{Sn)}$	5	2	^{152}La	20	
^{105}Y	12	7	$^{(118}\text{R.})$	3	2	^{137}Sb	548	164	$^{(153}\text{La)}$	5	
^{106}Zr	336	165	^{118}Rh	313	160	^{138}Sb	50	16	$^{(153}\text{Ce)}$	2	
^{107}Zr	38	21	^{119}Rh	82	30	^{139}Sb	8	3	^{154}Ce	9	
^{108}Nb	413	210	^{120}Rh	13	5	^{139}Te	1549	540	$^{(155}\text{Ce)}$	4	
^{109}Nb	81	41	$^{(121}\text{Rh)}$	3	1	^{140}Te	264	78			
^{110}Nb	10	6	^{121}Pd	211	150	^{141}Te	39	13			

The cross section of low energy fission has been evaluated from measured counting rates and using normalized elemental distribution (Fig.2). A value of 1.4 ± 0.1 b was obtained which is larger than the 1.1 b calculated for GR fission[10]. The difference can be attributed to the process which is filling the valley. However this larger cross-section is only a fraction of the 3.5 ± 0.3 b fission cross-section that we have measured at the same energy in the same experiment.

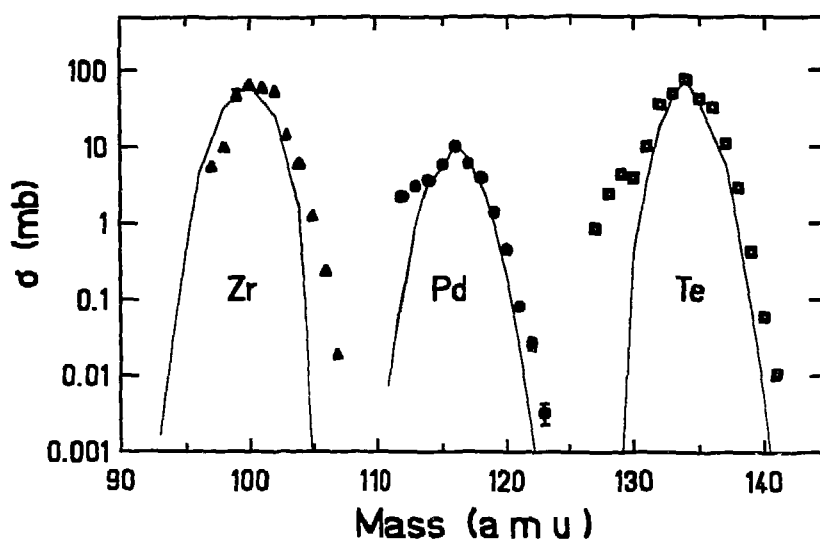
The element-yield distribution corrected for transmission effects (Fig. 2) leads to a peak-to-valley ratio of 6.4. This would indicate an excitation energy of 24 MeV for the fissioning U nucleus. However, the odd-even effect (5%) and shell effects which favour the production of the Zr-Te pair would indicate a low energy process with 10 MeV excitation. In order to further understand the reaction processes, isotopic yields for three elements were analysed: Pd ($Z = 46$) for symmetric fission in the valley of the Z distribution and the couple Zr-Te with complementary Z values 40 and 52 at the maximum of the elemental distribution. The result (Fig.5) shows almost Gaussian curves as well as in the case of thermal fission. The excess of yields obtained for the lightest isotopes results from the contribution of fission at higher excitation energies or from fission of lower mass projectile fragments. The mean values of the mass distributions carry some information on the processes: In case of Zr and Pd the mean mass of 100.6 and 134 adds to 234.6. Comparing to the standard values as tabulated for example by A. Wahl [11], we find for the Zr-Te couple $\nu=3.4$ neutrons emitted instead of 2.4 in thermal neutron fission. With the mean value of 116.0 for Pd mass distribution we find $\nu=6$ neutrons instead of 4.2. The difference in excitation energy compared to thermal neutron fission can be evaluated by the formulae $\Delta E_{ex} = \Delta v(B^A - \epsilon) - B^U$ in which B^A is the neutron binding energy in the fragment, ϵ its kinetic energy and B^U is the binding energy of the neutron captured in thermal n-fission of U. By taking values for those quantities from literature, we obtain 13 MeV from the Zr-Te pair and 22 MeV from Pd.

We conclude that at least two different fission mechanisms contribute to the measured low energy fission distributions: A process with an excitation energy of (10-12) MeV feeding the masses for asymmetric pairs, and a second process with an excitation energy of (22-24) MeV feeding the valley. The first would correspond to fission by virtual photons exciting the giant isovector resonances and the second to a very soft nuclear process.

The width σ_A of the mass distributions are found larger than for thermal fission or for p-induced fission [11]. Converting this width into a charge width by using $\sigma_Z = Z \Lambda_{mean} \sigma_A$, we obtain on the average, $\sigma_Z = 0.70 \pm 0.10$. The corresponding value in thermal neutron fission of ^{235}U is only 0.53. The larger width found here is difficult to understand. It might stem from a low energy fission process induced by one of the soft isovector modes. For future experiments this larger width can be exploited to populate isotopes even further from stability.

We have shown that using inverse kinematics all fragments created in relativistic collisions of ^{238}U on a lead target could be separated and identified unambiguously. The experimental method described here provides a novel and efficient way to study both qualitatively and quantitatively all processes which are taking place in those collisions. Note that those cross-sections on a light target need to be known precisely if accelerator boosted subcritical electro-

Fig. 5 Mass yields distribution of Zr, Pd and Te produced by low energy fission



nuclear devices were to be developed and brought to operation one day [12]. They are exactly the same as the one obtained in bombarding a U target with a relativistic proton beam.

The selection of the largest longitudinal momenta in collisions of U ions on a Pb target at relativistic energy provides a trigger on low energy fissions. At the incident energy of 180 GeV, the reaction does indeed exhibit features characteristic of low energy fission. More than forty new isotopes were discovered in this first measurement focussing on the light branch of fission products. Half-lives and mass-excesses become measurable since beam intensities have been recently increased by 2 orders of magnitude. Nuclear structure around the doubly magic ^{132}Sn and ^{78}Ni , and in the region of deformed nuclei can be investigated using Coulomb excitation of secondary fission fragment beams by the Cristal-Ball to be installed at GSI.

References

- [1] C. Wagemans, The nuclear fission process, CRC Press (1991)
- [2] M. Bernas et al., Phys. Rev. Lett. 67 (1991) 3661
- [3] H. Geissel et al Nucl. Instrum. Meth. B70 (1992) 286
- [4] T. J. M.Symons et al. Phys. Rev. Lett. 42 (1979) 40.
- [5] R.Anne et al. Nucl. Instr. and Meth. A257(1987)215
- [6] M.S. Antony: Chart of Nuclides-CRN Strasbourg (1992)
- [7] Th Schwab, GSI Report 91-10 (1991)
- [8] J. Äystö et al., Phys. Rev. Lett. 69 (1992) 1167
- [9] S. Czajkowski et al.. to be published in NIM
- [10] C. A. Bertulani and G. Baur, Phys. Rep. 163 (1988) 299
- [11] A.C. Wahl, A.N.D.T.39(1988)
- [12] Ch. Bowmann et al.. Nucl. Instr. and Meth. A320(1992)336
and C. Rubbia et al.. submitted to the same journal